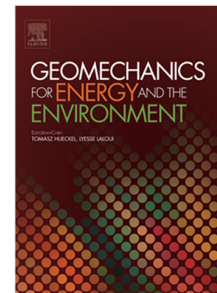# Journal Pre-proof

Thermal energy transfer around buried pipe infrastructure

I. Shafagh, P. Shepley, W. Shepherd, F. Loveridge, A. Schellart, S. Tait, S.J. Rees

Please cite this article as: I. Shafagh, P. Shepley, W. Shepherd et al., Thermal energy transfer around buried pipe infrastructure, *Geomechanics for Energy and the Environment* (2021), doi: https://doi.org/10.1016/j.gete.2021.100273.

This is a PDF file of an article that has undergone enhancements after acceptance, such as the addition of a cover page and metadata, and formatting for readability, but it is not yet the definitive version of record. This version will undergo additional copyediting, typesetting and review before it is published in its final form, but we are providing this version to give early visibility of the article. Please note that, during the production process, errors may be discovered which could affect the content, and all legal disclaimers that apply to the journal pertain.

Highlights

Highlights:

- A 30m long buried pipe was thermally activated by forced convection with hot water
- The pipe had a thermal influence extending over 4m ($>30D_{pipe}$) after 4 months
- Ambient conditions and adjacent pipes interact thermally with the buried water pipe
- Fluid in adjacent pipes can act as a heat sink due to induced convection
- Thermal diffusion dominates in the low moisture content sand around the pipe

Author Agreement

Author Agreement Statement

We the authors of the manuscript "Thermal Energy Transfer Around Buried Pipe Infrastructure":

1. Dr Ida Shafagh
2. Dr Paul Shepley
3. Dr Will Shepherd
4. Dr Fleur Loveridge
5. Dr Alma Schellart
6. Prof Simon Tait
7. Prof Simon Rees

declare that this manuscript is original, has not been published before and is not currently being considered for publication elsewhere.

We confirm that the manuscript has been read and approved by all named authors and that there are no other persons who satisfied the criteria for authorship but are not listed. We further confirm that the order of authors listed in the manuscript has been approved by all of us.

We understand that the Corresponding Author is the sole contact for the Editorial process. She is responsible for communicating with the other authors about progress, submissions of revisions and final approval of proofs.

Signed by Dr Ida Shafagh on behalf of all authors.

Dr Ida Shafagh; 25 May 2021

Thermal Energy Transfer Around Buried Pipe Infrastructure

I. Shafagh[a], P. Shepley[b], W. Shepherd[b], F. Loveridge[a], A. Schellart[b], S. Tait[b], S.J. Rees[a]

[a] University of Leeds, Leeds, UK
[b] University of Sheffield, Sheffield, UK

Abstract:

Decarbonisation of heating is essential to meet national and international greenhouse gas emissions targets. This will require adoption of a range of solutions including ground source heat pump and district heating technologies. A novel route to these solutions includes dual use of buried infrastructure for heat transfer and storage in addition to its primary function. Water supply and wastewater collection pipes may be well suited for thermal energy applications being present in all urban areas in networks already in proximity to heat users. However, greater understanding of their potential interactions with surrounding heat sources and sinks is required before full assessment of the energy potential of such buried pipe networks can be obtained. This paper presents an investigation into the thermal interactions associated with shallow, buried water filled pipes. Using the results of large scale experiments and numerical simulation it is shown that soil surface ambient conditions and adjacent pipes can both act as sources or sinks of heat. While conduction is the main mechanism of heat transfer in the soil directly surrounding any pipe, any adjacent water filled pipes may lead to convection becoming important locally. In the test case, the thermal sphere of influence of the water filled pipe was also shown to be large, at in excess of 4m over a timescale of 4 months. Taken together, these points suggest that design and analysis approaches when using water supply and wastewater collection networks for heat exchange and storage need careful consideration of environmental interactions, heat losses and gains to adjacent pipes or other infrastructure, and in ground conditions for a number of pipe diameters from any buried pipe.

1 Introduction

Heat provision represents around one third of all greenhouse gas emissions in the UK [1]. Therefore, to make substantial contribution to reductions in CO_2 emissions, delivering low carbon heat energy is an essential step. A promising and sustainable opportunity for low carbon heat energy is ground heat exchange and storage. However, factors such as high capital costs and adverse electricity and gas price ratios has slowed down uptake. A novel way to achieve affordable ground heat exchange is to use existing or new buried infrastructure for dual purposes: heat transfer along with the primary function. This significantly reduces capital costs and makes ground heat exchange and storage more economically feasible. It also provides opportunities to obtain heat direct from the infrastructure itself [2, 3].

One option for dual purpose infrastructure is heat recovery from urban water systems [4-6]. There are around 1 million kilometres of buried water supply and wastewater collection pipes in the UK, the vast majority of which are located within 1m of the ground surface [7]. A reliable and all-year-round energy source can be available within these buried pipes, which largely originates from domestic wastewater [8-10]. This provides an appealing opportunity for energy harvesting through retrofitting of ground heat exchange systems. These can take the form of additional heat transfer pipes installed adjacent to the

existing sewer mains. While shown to be practically viable, pilot studies suggest work to reduce capital costs is still required. Alternatively, when existing wastewater pipes are rehabilitated during future maintenance, this opportunity can be taken to add in-pipe lining systems which provide both strength and heat transfer elements. As well as these practical challenges, some technical challenges remain to be addressed [10, 11]. This includes the effects of ambient temperature variations, properties of the surrounding soil, and the thermal interactions of adjacent pipes.

To date studies investigating the potential of urban water networks as alternative sources of heating have focused on outlining its feasibility by investigating water temperature and flow rate trends in wastewater collection systems [9-16]. Nevertheless, such data are scarce. Frijns et al. [6] described how in the Netherlands, 60% of drinking water is heated in the house, and the temperature of wastewater leaving the house varies throughout the day and is on average 27°C. Measurements in Germany, Belgium, Switzerland, the Netherlands and Italy have found sewage temperatures to range up to 28°C [8-10, 17-19]. These relatively high temperatures of wastewater can potentially provide a significant amount of heat. Hao et al. [20] presented a theoretical potential of thermal energy of 4.64 kWh/m^3 for sewers based on an optimal extraction temperature of 4°C, which is similar to that reported by McCarty et al. [4]. However, the potential amount of heat recovery from sewer systems depends on other factors including efficiency of any connected heat pump system, distance between recovery and heat use locations, and boundary condition effects that could cause heat losses. Using the first law of thermodynamics and assuming 100% efficient heat recovery systems, Abdel-Aal et al. [9] estimated that if all UK wastewater could be lowered by 2°C, then the 11 billion litres of wastewater produced each day (as estimated by Defra [21]) could potentially result in 390 TWh of heat recovery per year.

Previous studies have also investigated in-pipe wastewater air interactions [22-24]. However, heat transfer analysis between such underground systems and their surrounding soils and adjacent pipes have mostly been unexplored [25-27]. For instance, it is known from work on retaining wall and tunnel ground heat exchangers that the heat capacity of buried infrastructure systems is strongly dependent on the internal and external thermal boundary conditions [28, 29]. Therefore, to develop heat recovery/storage solutions for buried pipe infrastructure requires further characterisation of the thermal exchange capacity between underground structures, the fluids within them and the surrounding soil. By better understanding the thermal exchange processes, any potential impact, when heat is recovered or stored, on the mechanical stability of the pipes or the performance of pipe networks in delivering their primary functions, can be quantified.

This study examines the thermal behaviour around piped urban water systems by examining the interactions at the thermal boundaries when the system experiences a temperature perturbation that could be caused by heat exchange and storage. First, details of the experimental and numerical analysis that have been performed on a system of several adjacent buried pipes installed in a large sand tank are

2

described in detail. Subsequently, the results are presented and the role of the boundary conditions and thermal interactions are explored. Finally, conclusions and recommendations are made for future work and practical application.

2 Experimental Design

A series of physical experiments were performed to investigate the heat transfer conditions around a series of buried water pipes. The important thermal interactions related to ambient air, water and pipe/soil interfaces have been studied over ranges representative of conditions in live water supply and wastewater collection pipes. The experimental system was designed to enable evaluation of the influence of ground and groundwater conditions, as well as in-pipe flow conditions, on the potential for heat transfer both within piped water infrastructure and to the surrounding ground. Experiments were carried out at the Integrated Civil and Infrastructure Research Centre (ICAIR) at the University of Sheffield. The experimental apparatus consists of a 4.5m × 2.8m × 30.0m tank (h*b*l), where its base and one wall are made of concrete and the other wall is steel (Figure 1 and Figure 2), filled with a fine silica sand of characteristics given in Table 1. The thermal properties of the sand were measured using KD2 Pro (transient line heat source method) with dual needle SH-1 probe at a range of different moisture contents, the results of which are shown in Table 2. Two sets of three 125 mm outer diameter (100mm internal diameter) HDPE pipes are installed at depths of 2.5m and 0.4m, where these values refer to the depth of the upper pipes (Figure 2), and all are filled with water throughout the experimental period.

At any one time during the experiments one of the six pipes was connected to a heating system to permit temperature perturbations to be applied to the system. The heating system comprised a large $2m^3$ header tank fitted with two 9kW electric immersion heaters, and an in-line circulation pump. Water was taken from the header tank, pumped through one of the buried pipes and then back into the header tank. Water temperature was controlled by varying heat input and sustaining the header tank temperature within 1°C of a target value. The header tank could be connected to any of the six buried pipes at a time and a constant recirculation water flow rate was achieved using an in-line pump and a flow control valve. For each temperature-flow rate condition, the parameters were held constant until temperatures in the soil surrounding the buried pipe reached a steady state, defined as no fluctuation greater than 0.1°C over 2 days. The results presented in this paper consider thermal activation of the deepest pipe in the lower cluster (2.74m below the surface) of three pipes (Figure 2b) while other pipes are filled with static water. After collection of background data, and circulation of water without direct heating, two heating periods were applied to the thermally activated pipe as summarised in Table 3. Due to the high flow rates used for the circulation, the temperature difference between inlet and outlet temperature of the activated pipe was close to the range of the sensor resolution, and therefore an average value of the water temperature has been presented in Table 3.

3

**Table 1.** Characteristics of sand used in the experiments

Particle Density	Sample Dry Density	Particle Size			Moisture Content	Porosity
		d10	d50	d95		
[Mg/m^3]	[Mg/m^3]	[mm]			[%]	
2.65	1.27	0.075	0.2	0.5	7	0.52

Table 2. Laboratory measurements of sand thermal properties

Moisture Content	Thermal Conductivity	Volumetric Specific Heat	Thermal Diffusivity
[%]	[W/mK]	[MJ/m^{3}K]	[mm^2/s]
25.0	1.92	2.20	0.87
20.0	1.80	1.97	0.91
14.2	1.62	1.74	0.93
10.0	1.45	1.56	0.94
5.0	1.14	1.38	0.83
2.5	0.36	1.11	0.33

Table 3. Thermal conditions during experimental programme at 7% moisture content

Stage	Detail	Duration (hrs)	Activated Pipe	
			Flow Rate (l/s)	Water Temperature (°C)
1	No heating; no water circulation	680	0	-
2	Water circulation with no heating	950	4.4	Variable, affected by ambient conditions
3	First heating	700	4.4	31
4	Second heating	620	4.4	43
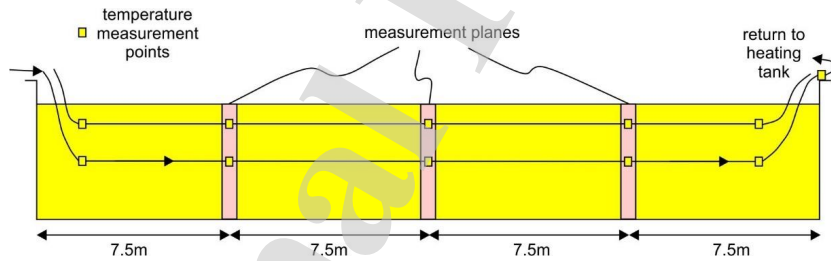
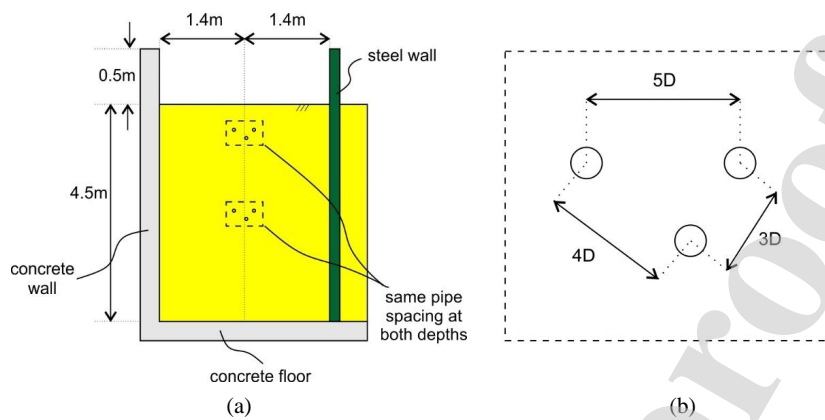**Figure 1.** Length-wise section of the experimental set up.

Figure 2. (a) Cross section of experimental set up; and (b) Pipe arrangements (distances between pipes ranging from 3 to 5 times the pipe diameter 'D').

The pipes and surrounding sand are instrumented to evaluate how thermal energy is transferred around heated pipes to the surrounding soil, or adjacent pipes. Instrumentation of the experiments permits soil temperature mapping, and hence calibration of system models. Thermocouples are installed on three instrumented planes for monitoring the pipe and ground temperatures in the experiment box as shown in Figure 1. Figure 3 shows their position in cross section relative to the pipes and experiment boundaries. This pattern is repeated at each plane. Additional sensors are also placed at the centreline of the tank's base, and at 0.9m and 3.0m depths on the four side boundaries. All thermistors were calibrated and are estimated to have a temperature measurement uncertainty of 0.1℃.
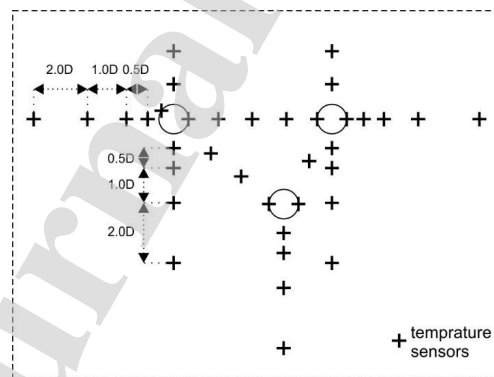

Figure 3. Local thermocouple positions adjacent to pipes (same positions at both depths, distances ranging from 0.5 to 4 times the pipe diameter 'D').

As the experiment was too large it had to be conducted in a large building without accurate environmental control. Ambient temperature conditions were thus monitored, primarily through additional thermocouples at the sand surface. These were complemented by the building's environmental control system which applied limited heating during winter to limit fluctuations in ambient temperature and relative humidity in the building environment. Variations in the surface boundary temperature were included in the numerical simulations.

The pipe water temperatures are monitored at several locations. Thermocouples are placed inside the pipe, on the external pipe walls, at the sand surface and inside the header tank used to heat the water. These are to ascertain the thermal exchange from the fluid to the external atmosphere through the pipe wall.

Fluid input temperatures have been systematically increased over the duration of the experiments from ambient initial conditions, in steps, to a maximum value of 43ºC. This embraces larger temperature range than expected in real urban water networks but allows some excitation of heat transfer to fully explore the significance of the various heat transfer mechanisms. The experimental facility, being essentially full-scale in cross section, has a time constant similar to a real system and so the experiments were carried out over several months, i.e. representative of the seasonal time scales of interest in real systems.

3   Numerical Approach

Numerical analyses were performed and validated using the experimental data. This permitted exploration of the key thermal processes affecting the system behaviour. There were limited temperature variations along the pipe connected to the heating system (refer to results presented in Section 4.1). This meant that a two-dimensional numerical analysis, using a vertical cross section of the system could be justified, Figure 4. The cell-centred finite volume method (FVM) as implemented in the *OpenFOAM* library was employed in the form of a conjugate heat transfer and fluid flow solver: *chtMultiRegionFoam*. *OpenFOAM* is an open-source package with variety of predesigned solvers for various types of applications of continuum mechanics [30]. Previous validated applications of *OpenFOAM* in ground heat transfer and storage include [31, 32].

To account for disparate continua comprising the domain shown in Figure 4 separate regions were defined in the simulations corresponding to sand, pipes and fluids. Such an approach with the solver in question allows a segregated solution strategy for different continuum/region in the domain, i.e. solving energy equation for all of the domain and also the Navier Stokes equations for liquids. However, full solution of the Navier Stokes equations is computationally expensive. Therefore, to substantially reduce the computational intensity of our simulations two alternative approaches were adopted for fluids in the domain. On both cases, forced convection is assumed within the thermal activated pipe, while two scenarios have been adopted for the pipes where the water is static. In one scenario (scenario #1) all

6

static water is treated as solid in the model for computational efficiency. This explicitly assumes no flow, either forced or due to temperature driven buoyancy effects, and initially appeared a reasonable assumption given no circulation was occurring and the temperature changes were known from monitoring data to be small. In a second scenario (scenario #2), convective boundary conditions are imposed on the inner surfaces of the two pipes in the embedded deeper cluster which are closest to the thermally activated pipe and therefore would experience some changes in temperature. While not subject to forced convection, the water in these pipes could theoretically experience some thermally driven water flow due to the temperature gradients leading to changes in fluid density along the pipes. This approach stops short of a full solution of the Navier Stokes equations, hence saving computational effort, but yet still allows for a small amount of buoyancy driven flow to be accounted for.

The governing equation in all regions of the numerical domain is the energy equation as shown in Equation 1 and the coupling at the interface between the regions is expressed using Equation 2:

$$\frac{\partial(\rho H)}{\partial t} = \frac{\partial}{\partial x_j}\left(\alpha\frac{\partial H}{\partial x_j}\right) \qquad \text{Eq. 1}$$

$$\lambda_f \frac{\partial T_f}{\partial n} = -\lambda_s \frac{\partial T_s}{\partial n} \qquad \text{Eq. 2}$$

where H is the specific enthalpy, ρ is the density and $\alpha = \lambda/C_p$ is the thermal diffusivity which is defined as the ratio between the thermal conductivity λ and the specific heat capacity C_p. In Equation 2 n represents the direction normal to the interface wall, T is the temperature while s and f denote solid and fluid respectively.
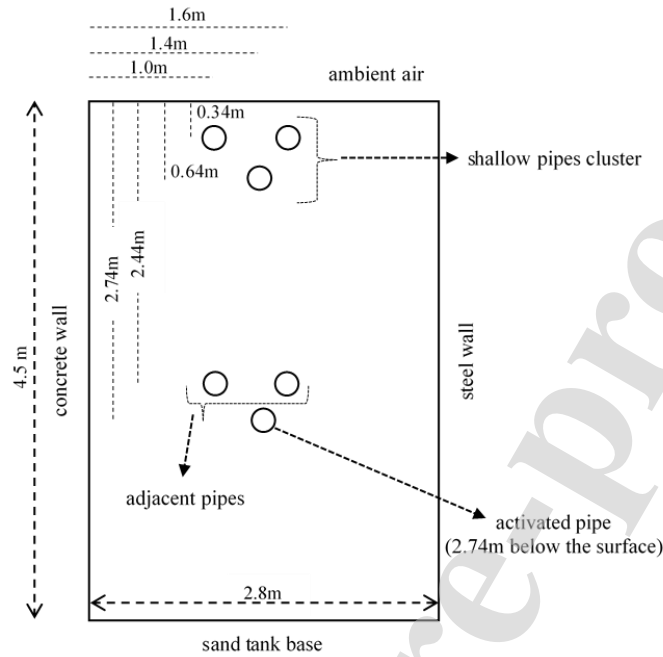
7

Figure 4. 2D representation of the investigated geometry.

3.1 Geometry and Meshing

The corresponding two-dimensional numerical domain is 4.5m by 3m in size, details of which are shown in Figure 4. It comprises three regions of sand, pipes, and fluids and is created and discretised using a combination of structured and unstructured meshing tools within *OpenFOAM* as illustrated in Figure 5, highlighting the boundary conditions. A relatively coarse structured mesh is applied over the entire region that is progressively reduced and switched into unstructured mesh towards regions where higher temperature gradient is expected, i.e. pipes and their corresponding interfaces. Mesh independence analysis have been carried out to verify satisfactory geometrical mesh and grid independence of the numerical results. The total number of grid cells for the domain was about 10^6 ranging from 2.7×10^{-7} m^2 to 0.09 m^2 in size.
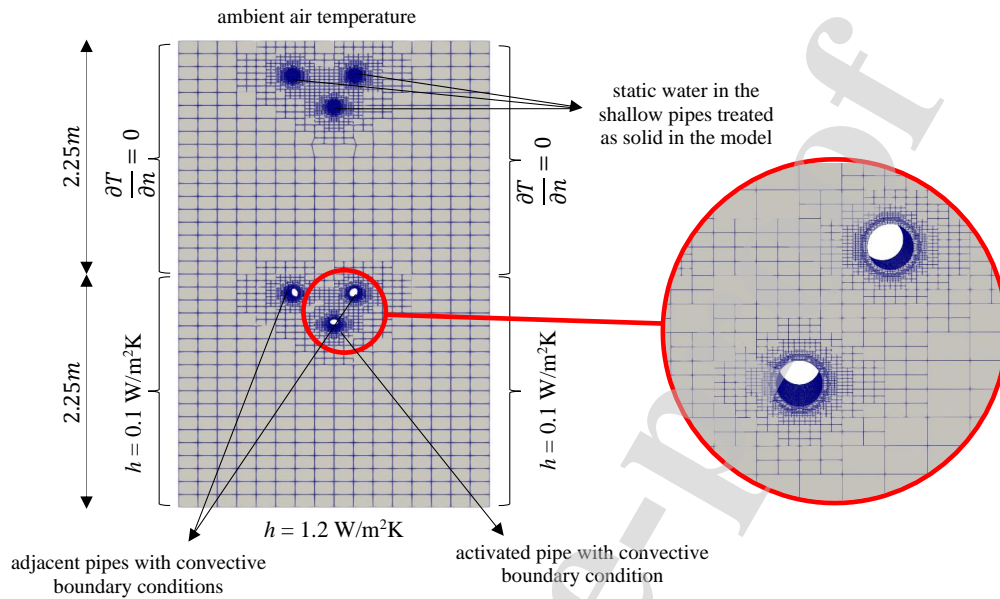
Figure 5. Grid representation of the sand tank, the embedded pipes, and the fluid regions, highlighting the imposed boundary conditions. Note that the 2D model includes one element depth as shown in the inset.

3.2 Materials Thermal Properties

Material properties relevant to heat transfer analysis are the thermal conductivity, specific heat capacity, and density. The properties for sand in the numerical model are implemented using data in Table 2 that are derived from in-situ measurements showing 7% moisture content. It should be noted that thermal properties of sand are highly dependent on its water content, which can significantly affect the heat transfer through this region [33]. Table 4 details the thermal properties of the materials used in the simulation.

Table 4: Materials' properties used in numerical analysis

	Sand (7% moisture content)	Water	Pipe
Thermal Conductivity [W/mK]	1.26	0.63	0.40
Specific Heat Capacity [J/kgK]	890.61	4186.00	1900.00
Density [kg/m³]	1630.00	1000.00	970.00

3.3 Initial and Boundary Conditions

3.3.1 Pipes

Forced convection is assumed within the thermally activated pipe, for which the heat transfer coefficient for the flowing water, h_f, is determined using the Gnielinski correlation [34, 35] as shown in Equation 3:

9

$$h_f = \frac{\lambda_f \left(f/8 \right) (Re - 1000) Pr}{2r_p \left[1 + 12.7 \left(f/8 \right)^{1/2} (Pr^{2/3} - 1) \right]}$$

Eq. 3

where λ_f is the thermal conductivity of the fluid, here water, f is the Darcy-Weisbach friction factor, Re is the Reynolds Number, and Pr is the Prandl Number as defined through Equations 4 to 6 respectively. The Gnielinski correlation is valid for $0.5 \leq Pr \leq 2000$ and $3000 \leq Re \leq 5 \times 10^6$. Considering this Reynolds Number validity range, Eq. 3 is only used for turbulent flow simulations.

$$f = (0.79 \ln(Re) - 1.64)^{-2}$$

Eq. 4

$$Re = \frac{4Q}{\pi \nu D}$$

Eq. 5

$$Pr = \frac{C_p \mu}{\lambda_f}$$

Eq. 6

In Equations 5 and 6, D is the pipe inner diameter and ν and μ are the kinematic and dynamic viscosities of the fluid respectively. Average fluid temperature in each stage of the experiment was used to derive values for variables applied to determine h_f for the four stages of the experiment, these values along with the calculated h_f are detailed in Table 5.

Table 5. Values used in Equation 3 to calculate the heat transfer coefficients

$T_{average}$ °C	Cp [J/kgK]	μ [kg/ms]	λ_f [W/mK]	ν [m²/s]	Re	Pr	f	h_f [W/m²K]
13.6	4186	1.18×10^{-3}	0.586	1.18×10^{-6}	4.69×10^4	8.427	2.13×10^{-2}	1952
18.4	4186	1.04×10^{-3}	0.595	1.04×10^{-6}	5.32×10^4	7.320	2.07×10^{-2}	2084
33.0	4186	7.49×10^{-4}	0.617	7.53×10^{-7}	7.37×10^4	5.075	1.92×10^{-2}	2441
43.0	4186	6.13×10^{-4}	0.631	6.19×10^{-7}	8.96×10^4	4.060	1.84×10^{-2}	2667

Consequently, the forced convection boundary condition on the thermal activated pipe is applied in the model using Equation 7:

$$\lambda_s \frac{\partial T}{\partial n} + h_f (T - T_f) = 0$$

Eq. 7

where T_f is the time dependant flowing fluid temperature. In the scenario where convective boundary conditions are also imposed on the inner surfaces of the two pipes adjacent to the thermal activated pipe (scenario #2), very small convection heat transfer coefficients, 30 Wm^{-2}K^{-1}, together with a constant fluid temperature equal to the initial condition is used for all stages of the study. This approach was taken to represent laminar flow conditions in these pipes.

3.3.2   Outside Boundaries

Recorded ambient temperature variations are imposed on the model top surface of the sand tank while a mixed boundary condition is imposed on the base of the sand tank as well as the lower half of the side

10

walls to represent heat transfer through these surfaces. This type of boundary condition allows heat flux on the external walls through specifying a fixed heat transfer coefficient and adjacent temperature. The upper half of the side walls are given a zero heat flux condition, i.e. $\frac{\partial T}{\partial n} = 0$. These choices of boundary conditions along with suitable values of the heat transfer coefficient imposed on the external walls are based on a series of calibration analyses to identify the appropriate boundary condition types for the domain (refer to Section 4). This choice of boundary conditions was applied after initial investigation showed that temperature changes from the ambient interface within the experimental facility are more important in the upper half of the side walls, while lateral heat losses dominate beneath this point.

3.3.3   Initial Conditions

The initial temperatures of all materials and boundaries are assigned based on the corresponding experimental values.

4   Results

4.1   Experimental Results

The variation of the upstream and downstream temperatures in the thermally activated pipe are shown in Figure 6 for the full duration of the experiment. Since the experiment was undertaken in the spring and summer a trend of generally increasing ambient air temperature within the experimental facility can be seen. Superimposed on this trend are the specific daily variations. Since no heat input (with the exception of the small amount of pumping energy) occurs until around 1630 hours from commencement, it can be seen that the ambient air temperature variations have a strong influence on various parts of the system. Between the commencement of the test and the start of the first heating phase, the ambient air temperature increases by approximately 5°C. Within the sand tank the increase in temperature is more modest, falling from 4°C at 0.9m depth, to 1.5°C at 3m depth and to 1°C at the base of the tank (4.5m depth). This shows the expected diminishing impact of the surface conditions at greater depth, but none the less confirms its influence even to the base of the experiment.

Meanwhile, the thermally activated pipe, which is embedded at 2.74m depth, changes temperature prior to heating by approximately 4°C. This change largely corresponds with the changes in ambient conditions and is a reflection that (i) the header tank is in likely equilibrium with its environment, and (ii) the surface pipework between the header tank and the point the pipe enters the sand is not completely insulated. Additionally, the small increase in the fluid temperature above ambient temperature during initial circulation may reflect heat input from pumping. After the commencement of the first heating phase, stage 3 in Figure 6, the temperature of the water in the thermally activated pipe increases to reflect that of the now heated water in the header tank. As the tank is no longer in equilibrium with the surrounding air, the water is proportionally less influenced by ambient conditions. In these two last phases of the test, i.e. stages 3 and 4, the temperature at the base of sand tank and at greater depth also

11

shows an acceleration of temperature increase. This reflects the fact that some of the heat injected into the system is being lost at the side and base boundaries.

From about 2150 to 2320 hours the flow rate was reduced to 0.42 l/s in an attempt to investigate laminar flow conditions, however, the system was unable to maintain a stable flow and the minimal flow rate in the tank resulted in a lack of mixing which meant the PID controller was unable to maintain a steady temperature, as shown in Figure 6. After the increase to 43°C, there remained some small high frequency fluctuations in the temperature due to the limitations of the temperature control system.
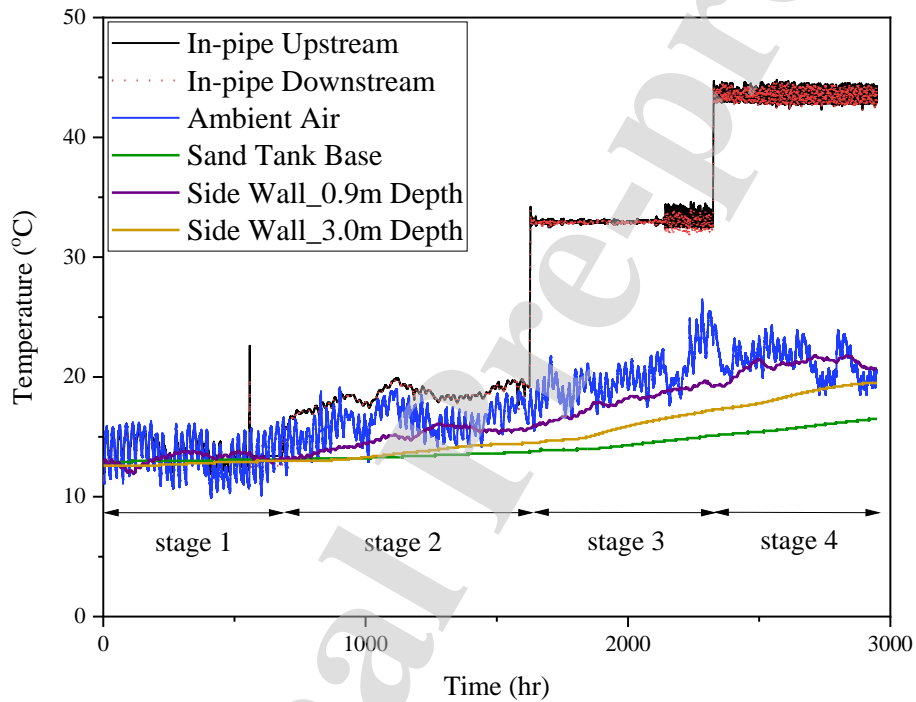

Figure 6. Variations of ambient air, activated pipe upstream and downstream and external tank boundary temperatures.

4.2 Simulation Results

4.2.1 Calibration

The initial sample of the experimental data, prior to heating, were used to calibrate the model boundary conditions. Initially all the side walls and the tank base were prescribed with a zero heat flux boundary condition while the top surface was exposed to ambient air. This allowed examination of the effect of ambient air temperature on heat transfer in various parts of the domain as well as confirming the appropriateness of the thermal properties of the sand used in the model. Ambient air temperatures were observed to dominantly control temperature variations in the system over the first and second stages of

12

the analysis (corresponding to stages 1 and 2 of the experiments as shown in Figure 6), particularly at shallow depths. Meanwhile in deeper locations, heat losses at the sides and base clearly became more important, especially in the first and second heating stages, i.e. stages 3 and 4 in Figure 6. Therefore, the thermal boundary conditions were switched to use (i) heat flux boundary conditions to allow for heat transfer through the lower parts of the domain including the tank base and the lower part of the side walls, and (ii) an adiabatic boundary condition over the upper half of the side walls. This proved a more appropriate representative of the heat losses effecting the tank. By a process of calibration to minimise the difference between measured and simulated temperatures on these boundaries, the values of heat transfer coefficient for the heat flux boundaries on base and lower half of the sidewalls were fixed at 1.2 and 0.1 $Wm^{-2}K^{-1}$ respectively, while the initial condition was used as the external surface temperature. This approach seems reasonable given the initial thermal conditions of the building substructure and its properties are uncertain. These values were used for all stages of the simulation.

A comparison between the experimental and numerical analysis for temperature variations along the walls and the tank base with the described arrangements are shown in Figure 7(a)-(d) and Figure 8. Modifying the side walls boundary conditions to allow for heat transfer through the lower parts of the domain including tank base and side walls, as shown in Figure 5, resulted in better agreement between numerical simulations and experimental results compared to adiabatic boundary conditions, which emphasizes the significance of heat loss to the base and sides of the tank over this timescale despite its large size.
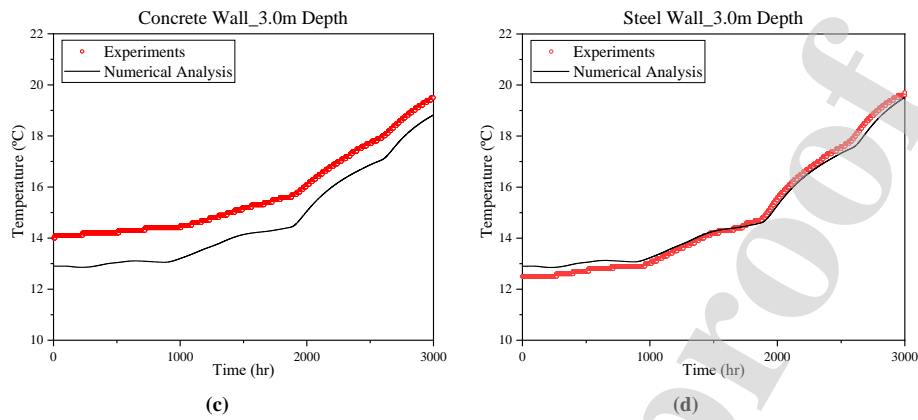

(a)   (b)

13
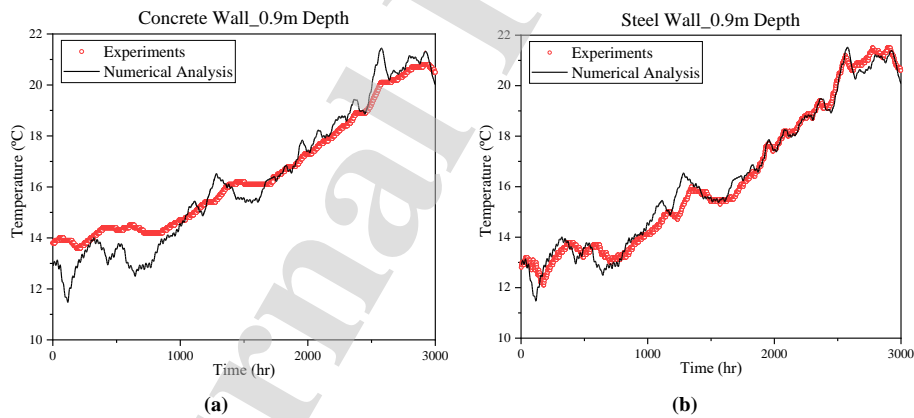
Figure 7. Comparison of the numerical and experimental temperature variations on the side walls of the sand tank at different depths. All numerical analysis refer to scenario #2, where adjacent pipes to the activated pipe are given convective boundary conditions.
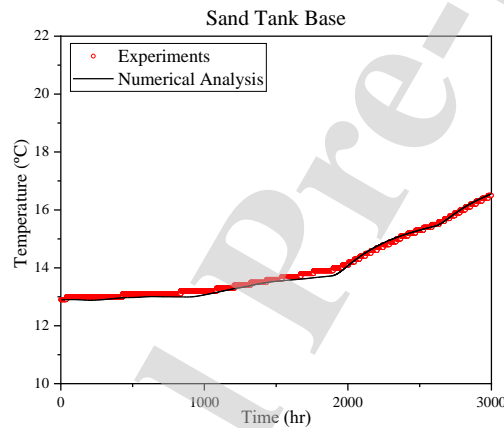

Figure 8. Comparison of the numerical and experimental temperature variations on the sand tank base. Numerical analysis refer to scenario #2, where adjacent pipes to the activated pipe are given convective boundary conditions.

4.2.2 Pipe Interactions

Two scenarios are presented in Figures 9(a) to 9(d). The case where a convective boundary condition is applied only to the thermally activated pipe (scenario #1), with the two adjacent pipes treated as purely conductive to reduce computational time, and the case where all three pipes in the lower cluster have convective boundary conditions at their internal surface (scenario #2). In the latter case low values are assumed for very small flow rates. It can be seen that a good match to the experimental data can only be obtained when interactions are accounted for with the adjacent pipes, even though there is no flow imposed on the water within these pipes. Otherwise, neglecting these heat losses, results in much

14

higher temperature prediction at and near the thermally activated pipe. Temperature distributions for scenario #2 within the domain across the four stages of the analysis are illustrated in Figure 10.
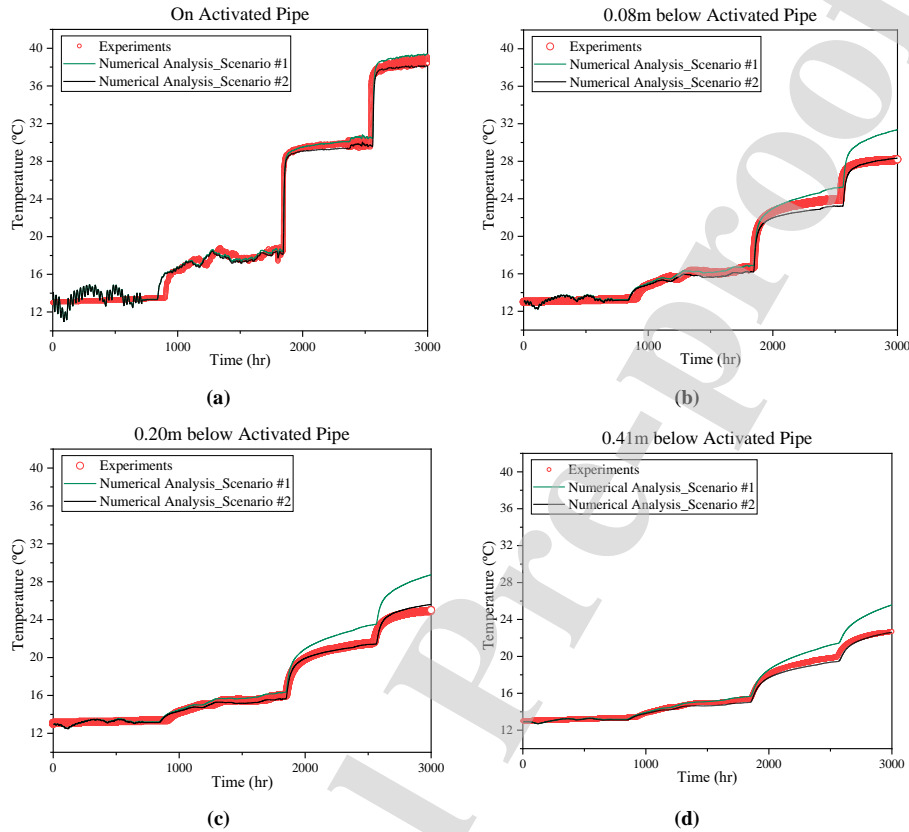

(a)   **(b)**

(c)   **(d)**

Figure 9. Comparison of the numerical and experimental temperature variations on the activated pipe and below it at different depths. Scenario #1 refers to where the static water in the pipes are treated as solid, and scenario #2 is where the two adjacent pipes to the activated pipe are given convection boundary conditions.
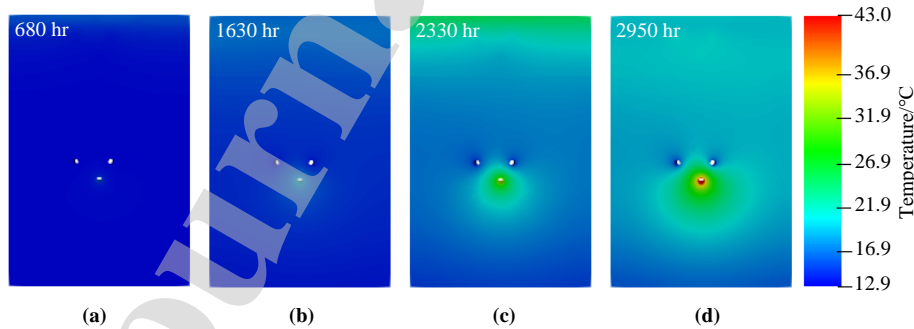

(a)   **(b)**   **(c)**   **(d)**

Figure 10. Variations of temperature distribution in the domain at four stages of the analysis for scenario #2.

15

5   Discussion

5.1   Implications for Heat Exchange and Storage

When seeking to understand the thermal processes operating around a heated buried water pipe it is important to consider both the key mechanisms of heat transfer and the impact of boundary conditions and other interactions. The sand tank simulation results support the suggestion that the main heat transfer mechanisms in the surrounding soils was conduction. While theoretically the materials used and the low moisture content (measured to be around 7%, or degree of saturation of 17%) suggest that there could be some scope for thermal redistribution of moisture (Figure 11), no evidence could be found for this. While we were not able to test for moisture content close to the thermally activated pipe after the test was complete, numerical investigation did not suggest any significant effect. Specifically, consideration of a lower thermal conductivity material near the thermally activated pipe during the later test stages did not improve the simulation fit to the experimental data. However, this may not be the case for all ground conditions, and smaller grain sizes with high degrees of saturation could be susceptible to enhanced heat transfer and soil drying due to heat injection. Additionally, real water pipe networks are likely to extend across different soil types and degrees of saturation where a range of behaviours could be expected.
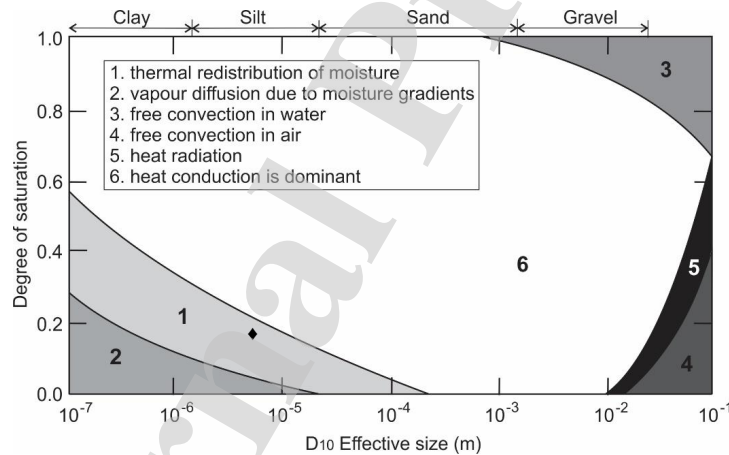

Figure 11. Predominant heat transfer mechanisms by grain size and saturation (after Loveridge [36] redrawn from Farouki [37]). ♦ shows the condition of the sand used in the experiments.

The second major aspect highlighted by this study is the importance of boundary conditions and pipe interactions. Even in a relatively large sand tank (4.5m × 2.8m × 30.0m), once long enough timescale experiments are conducted the boundaries are seen to influence the results. In this case accounting for the lateral and basal heat losses were important to matching the results with simulation. For a real

16

scheme to use water pipe networks for thermal exploitation this means that in the timescale of use (inter-seasonal storage and/or extraction) the zone of influence of any thermal activated pipe is quite large. Consequently any analysis or design approach needs to consider not just trench backfill materials, but local geology and ground water conditions and any other sources or sinks of heat within that zone. Since many pipes are at shallow depths, the inclusion of ambient interference in any analysis is therefore essential.

Furthermore, many water, wastewater and other utility infrastructure installations are found within close proximity to each other in practice. The results of these experiments demonstrate that these could all act as additional heat sinks. In the experiment presented, the water in the adjacent pipes was static but, in practice, it is likely that any heat losses or gains would be amplified by forced convection. Electrical cables are also well known as a source of heat [38] and so may be considered in the heat transfer analysis as well as potentially provide additional resources that could be harvested by near-by water and wastewater pipes.

5.2 Implications for Further Work

The experiment presented is one of the first such large scale trials of heating extraction or injection related to buried pipe networks. As such it highlights a number of areas where further valuable experimental data could be gathered in extensions to the work.

Due to a combination of pipe flow rates and temperature sensor accuracy the difference in temperature between upstream and downstream conditions was relatively small. For future assessment of energy potential from water pipelines consideration of the heat losses along the pipeline rather than just perpendicular to it will be required. This important aspect has been outside of the scope of this present study but will need to be addressed in future work. Lessons in this regard may be learned from the analysis and modelling of district heating networks [31].

The perimeter heat losses indicated in this study were found to be of some significance. Further experimental work, or numerical assessment will either need to take into account an even larger domain, or preferably facilitate measurement of heat fluxes at experiment boundaries to avoid the need for model calibration. For experiments at full scale in the field, this also suggests the need for accompanying temperature sensors to be several meters from any activated pipes.

Finally, to confirm the principal means of heat transfer, inclusion of water content and/or thermal conductivity sensors within the experiment domain would be beneficial to monitor whether there are noticeable changes to moisture conditions as a result of thermal processes.

6 Conclusions

Experimental and numerical analysis were carried out to investigate the thermal regime in a system of buried pipes where one pipe was thermally activated. Our results demonstrate that:

17

- For the low moisture content fine sand used in the investigation, thermal conductivity is the dominant heat transfer mechanism. No evidence of moisture movement was ascertained.
- Despite burial of the pipes at about 2.5m depth, the ambient environmental interactions were important. While the temperature changes caused by ambient effects were small in this case compared with the heat injected in the relatively warm ambient conditions, heat gained or lost to the environment will need to be accounted for when considering both summer and winter conditions.
- Although only the deepest pipe in the system was activated, the presence of fluid in two adjacent pipes were found to have an important effect on the heat transfer process from the activated pipe highlighting that other activity in urban environment will influence pipe thermal behavior.
- Even for the 2.8m wide sand tank used over the 4 months of the experiment significant heat losses occurred to the sides and base of the tank.

Taken together these conclusions suggest that design and analysis approaches for water and wastewater pipe networks used for heat exchange and storage need careful design. This should consider environmental interactions, heat losses and gains to adjacent pipes or other infrastructure, and in ground conditions for a number of meters from the buried pipes. While these interactions are able to be captured by a 2D diffusion simulation, less computationally demanding 3D analysis methods will be required for full pipelines. Whether non-diffusive simulations of ground thermal processes could also become important in certain scenarios also remains to be investigated.

7 Acknowledgements

8 References

[1] Emissions from Heat: Statistical Summary, 2012, Department of Energy &Climate Change, UK.
[2] A. Mortada, R. Choudhary, K. Soga, 2018, Multi-dimensional simulation of underground subway spaces coupled with geoenergy systems, J Build Perform Simul, 11(5), 517-537.
[3] F. Loveridge F, J.S. McCartney, G.A. Narsilio, M. Sanchez, 2020. Energy geostructures: A review of analysis approaches, in situ testing and model scale experiments. Geomechanics for Energy and the Environment, 22, 100173.
[4] P.L. McCarty, J. Bae, J. Kim, 2011, Domestic wastewater treatment as a net energy Producer—can this be achieved? Environ. Sci. Technol., 45, 7100-7106
[5] O. Nowak, P. Enderle, P. Varbanov, 2015, Ways to optimize the energy balance of municipal wastewater systems: lessons learned from Austrian applications, J. Clean. Prod., 88, 125-131.

[6] J. Frijns, J. Hofman, M. Nederlof, 2013, The potential of (waste) water as energy carrier, Energy Convers Manag, 65, 357-363.

[7] R. Long, 2018, Private correspondence, Acoustic Sensing Technology Ltd, May 2018.

[8] R.P.S. Schilperoort, F.H.L.R. Clemens, 2009, Fibre-optic distributed temperature sensing in combined sewer systems, Water Sci. Technol., 60, 1127–1134.

[9] M. Abdel-Aal, A. Schellart, S. Kroll, M. Mohamed, S. Tait, 2018, Modelling the potential for multi-location in-sewer heat recovery at a city scale under different seasonal scenarios, Water Research, 145, 618-630.

[10] S.S. Cipolla, M. Maglionico, 2014, Heat recovery from urban wastewater: analysis of the variability of flow rate and temperature, Energy & Buildings, 64, 122-130.

[11] G. Neugebauer, 1, F. Kretschmer, R. Kollmann, M. Narodoslawsky, T. Ertl, G. Stoeglehner, 2015, Mapping Thermal Energy Resource Potentials from Wastewater Treatment Plants, Sustainability, 7(10), 12988-13010

[12] F. Kretschmer, L. Simperler, T. Ertl, 2016, Analysing wastewater temperature development in a sewer system as a basis for the evaluation of wastewater heat recovery potentials, Energy and Buildings, 128, 639-648.

[13] X. Guo, M. Hendel, 2018, Urban water networks as an alternative source for district heating and emergency heat-wave cooling, Energy, 145, 79-87.

[14] Y. Gu, Y. Li, X. Li, P. Luo, H. Wang, Z.P. Robinson, X. Wang, J. Wu, F. Li, 2017, The feasibility and challenges of energy self-sufficient wastewater treatment plants, Applies Energy, 204, 1463-1475.

[15] J.A. Elías-Maxil, Jan Peter van der Hoek, Jan Hofman, Luuk Rietveld, 2014, Energy in the urban water cycle: Actions to reduce the total expenditure of fossil fuels with emphasis on heat reclamation from urban water, Renewable and Sustainable Energy Reviews, 30, 808-820.

[16] D. Cecconet, J. Raček, A. Callegari, P. Hlavínek, 2020, Energy Recovery from Wastewater: A Study on Heating and Cooling of a Multipurpose Building with Sewage-Reclaimed Heat Energy. Sustainability, 12, 116.

[17] W. Bischofsberger, C.F. Seyfried, 1984, Wärmeentnahme aus Abwasser (Heat Extraction from Wastewater), Lehrstuhl und Prüfamt für Wassergütewirtschaft und Gesundheitsingenieurwesen der Technischen Universitat München, Garching.

[18] D.J. Dürrenmatt, O. Wanner, 2008, Simulation of the wastewater temperature in sewers with TEMPEST. Water Sci. Technol. 57 (11), 1809-1815.

[19] L. Simperler, 2015, Impact of Thermal Use of Wastewater in a Sewer on the Inlet Temperature of a Wastewater Treatment Plant. Master's Thesis. University of Natural Resources and Life Sciences.

[20] X. Hao, J. Li, M.C. Van Loosdrecht, H. Jiang, R. Liu, 2019, Energy recovery from wastewater: Heat over organics, Water Res., 161, 74–77.

[21] DEFRA, 2012, Waste water treatment in the United Kingdom – 2012 Implementation of the European Union Urban Waste Water Treatment Directive – 91/271/EEC.

[22] M. Abdel-Aal, S. Tait, M. Mohamed, A. Schellart, 2021, Using long term simulations to understand heat transfer processes during steady flow conditions in combined sewers, Water, 13, 570.

[23] D.J. Durrenmatt, O. Wanner, 2014, A mathematical model to predict the effect of heat recovery on the wastewater temperature in sewers. Water Res., 48(1), 548–558.

[24] J.A. Elías-Maxil, J. Hofman, B. Wols, F. Clemens, J.P. Van Der Hoek, L. Rietveld, 2017, Development and performance of a parsimonious model to estimate temperature in sewer networks. Urban Water J., 14, 829–838.

[25] T. Kusuda, 1975, Heat transfer studies of underground chilled-water and heat- distribution systems, Proc. Symposium on Underground Heat and Chilled- Water Distribution Systems, Washington, DC, 1973. Report No. NBS-BSS- 66, 18-41.

[26] D. Fuertbauer, C. Cheng, 2019, Investigation of the influence on the heat transferred from a pipeline to the ground due to the presence of adjacent pipelines using Finite Element Method, 16th Pipeline Technology Conference, Germany, March 2019.

[27] A. Oosterkamp, T. Ytrehus, S.T. Galtung, 2016, Effect of the choice of boundary conditions on modelling ambient to soil heat transfer near a buried pipeline, Appl Therm Eng, 100, 367-377.

[28] P.J. Bourne-Webb, T.M. Bodas Freitas, R.A. da Costa Gonçalves, 2016, Thermal and mechanical aspects of the response of embedded retaining walls used as shallow geothermal heat exchangers, Energy Build.

[29] N. Makasis, G.A. Narsilio, A. Bidarmaghz, I.W. Johnston, Y. Zhong, 2020, The importance of boundary conditions on the modelling of soldier pile retaining walls as energy geo-structures, Computers and Geotechnics, 120.

[30] H. G. Weller, H. Jasak, G. Tabor, 1998, A tensorial approach to computational continuum mechanics using object-oriented techniques. Computers in Physics, 12, 620–631.

[31] S.S. Meibodi, S.J. Rees, D. Yang, 2019, Modelling the Dynamic Thermal Response of Turbulent Fluid Flow Through Pipelines, Proceedings of Building Simulation 2019: 16th Conference of IBPSA.

[32] S.Sandler, B. Zajaczkowski, B.Bialko, Z.M. Malecha, 2017, Evaluation of the impact of the thermal shunt effect on the U-pipe ground borehole heat exchanger performance. Geothermics, 65, 244–254.

[33] S.J. Rees, 2016, Advances in Ground-Source Heat Pump Systems, vol. 53. Elsevier Ltd.

[34] V. Gnielinski, 1975, Neue Gleichungen für den Wärmeund den Stoffübergang in turbulent durchströmten Rohren und Kanälen. Forsch. Ingenieurwes, Engineering Research, 41, 8-16.

[35] V. Gnielinski, 1976, New equations for heat and mass transfer in the turbulent pipe and channel flow. Int. Chem. Eng. 16, 359-368.

[36] F. Loveridge, 2012, PhD Thesis: The thermal performance of foundation piles used as heat exchangers in ground energy systems. Univ Southhampton 206pp.

[37] O.T. Farouki, 1986, Thermal properties of soils, series on rock and soil mechanics, Vol. 11, Trans Tech Publications, Germany.

[38] G. Davies, A. Revesz, G. Maidment, Alex Davenport, B. Yazadzhian, 2019, Electrical cable tunnel cooling combined with heat recovery, in cities, CIBSE Technical Symposium, Sheffield, UK 25-26 April.

20

CRediT Author Statement

I.   I. Shafagh: Methodology, Software, Validation, Formal analysis, Writing – Original Draft, Visualization

II.   P. Shepley: Writing – Review & Editing, Methodology, Investigation, Funding Acquisition

III.   W. Shepherd: Writing – Review & Editing, Investigation, Data Curation

IV.   F. Loveridge: Writing – Review & Editing, Conceptualization, Methodology, Supervision, Funding Acquisition

V.   A. Schellart: Writing – Review & Editing, Funding Acquisition

VI.   S. Tait: Writing – Review & Editing, Conceptualization, Methodology, Supervision, Funding Acquisition

VII.   S.J. Rees: Writing – Review & Editing, Conceptualization, Methodology, Supervision, Funding Acquisition

Declaration of interests

☒ The authors declare that they have no known competing financial interests or personal relationships that could have appeared to influence the work reported in this paper.

☐ The authors declare the following financial interests/personal relationships which may be considered as potential competing interests: